

# On potential use of natural electromagnetic emissions in ELF, VLF and HF radio bands at active landslide areas: Preliminary results from Vinohrady nad Váhom site (Slovakia)

Michal HOFFMAN<sup>1,2</sup> 

<sup>1</sup> Earth Science Institute, Slovak Academy of Sciences,  
P.O. Box 106, Dúbravská cesta 9, SK-840 05, Bratislava, Slovak Republic;  
e-mail: hoffman2@uniba.sk

<sup>2</sup> Comenius University in Bratislava, Faculty of Science, Department of Engineering Geology, Hydrogeology and Applied Geophysics,  
Mlynská dolina, Ilkovičova 6, 842 15 Bratislava, Slovak Republic

**Abstract:** The use of natural electromagnetic (EM) emissions in extreme low frequency (ELF) and very low frequency (VLF) radio bands for monitoring and predicting landslide activity is examined. The approach is based on measuring EM emissions using radio receivers and subsequent correlation of their intensity with the amount and character of deformation in the landslide. There are several sources of EM emissions in the rock environment, but it is mostly the piezoelectric impulse of quartz grains during the deformation or sliding movements within rock masses. Deformation was observed in the studied landslide body. Deformations were measured using a geodetic band and a network of stakes, which were installed before and re-measured after recording a natural EM signal attributed to the geodynamic activity. A method of direct monitoring of the entire VLF spectrum using sound cards such as AD converters was applied. So far, several candidate signals were captured and two permanent VLF monitoring stations have been built.

**Key words:** geodynamics, radio emission, very low frequency, landslides, piezoelectromagnetic

## 1. Introduction

Natural radio emissions, which are part of electromagnetic (EM) emissions in the radio band, in our research from 100 Hz to 30 MHz, i.e., ELF, VLF and HF, arise from atmospheric changes, atmospheric discharges, aurora borealis, as well as geomagnetic and solar storms. They also originate from some geodynamic phenomena, such as earthquakes, avalanches, active shear

zones, but also slope creep and landslides or rock falls. They may be emitted before, during or after such events (*Kharkhalis, 1995*). Research on natural radio emissions provides a new perspective to study these geodynamic phenomena. Monitoring and interpretation of these phenomena is complicated by a number of different artificial (antropogenic) signals from radio stations and networks of mobile operators, but also by several natural signals caused by solar processes and geomagnetic storms. The presented work focuses on slope landslides.

Active slope displacements generate continuous or pulsed (PEE) EM emissions caused by voltage in the sliding body or friction on the sliding surface (*Maniak, 2015; Hayakawa, 2015*). These emissions can sometimes last and be recorded for several days before observable deformation or before sudden detachment occurs at the landslide area. The maximum intensity of these emissions is in the frequency band 1–50 kHz (*Mastow et al., 1989a; Blaha and Duras, 2004; Kharkhalis, 1995; Fabo et al., 2004; Vybiral, 2002*). Pulse PEEs are measured in units of PPS (pulses per second). These emissions are measured by means of a receiving apparatus consisting of a receiver located in a well or borehole in the landslide area and a secondary receiver, which serves to eliminate EM emissions of sources other than those originating in the monitored landslide. For very fast moving slides, only one receiver is used, which is shielded. The number of pulses (PPS) is proportional to the intensity of the sliding process (*Mastow et al., 1989a*).

In the PEE method, the detector (picoteslameter) in the measuring system detects the vertical components of the magnetic field ( $B_z$ ). The direct current (DC) value represents the value of  $B_z$  on the connected multimeter is negligible due to the symmetry of the problem, if the conductive layer is mostly or nearly horizontal. But the fluctuations of the current density in the conductive layer produce an alternating current (AC) with corresponding magnetic field with non-zero  $B_z$  component. Assuming that the conductive layer lies in the  $x-y$  plane and that each surface element  $dA = dx \cdot dy$  contributes to the magnetic field  $B$ , the contribution to the  $B_z$  component can be easily obtained from Biot-Savart's law.

Once the spectral density is calculated, the measured root mean square (RMS) value of the random AC magnetic field can be obtained using the relation (*Jarošević and Kundráčik, 2004*):

$$B_{zRMS}[T] = \sqrt{S_{B_z} \cdot \Delta f}, \quad (1)$$

where  $S_{Bz}$  is spectral density and  $\Delta f$  is bandwidth of measuring system.

The measurement of PEEs in wells or on the surface experiences many problems due to many interfering signals which can pass through the filter with sufficient intensity and can be mistakenly assigned to natural sources of impulses. The antenna system used in the measurements of PEEs is also omnidirectional, i.e., it receives unwanted noise even when the position of the antenna changes. The air-loop antenna we use is strongly directional, which allows us to directly target the source of EM emissions and eliminate the ambient radio-frequency (RF) EM noise. The main sources of EM emissions at active landslide are: the piezoelectric effect, crack formation (Fig. 1), the streaming potential and the tribo-electricity (*Lowell and Rose-Innes, 1980*). The piezoelectric phenomenon is dominant at landslides with descending masses of sandy and gravelly fraction containing rock fragments the size of stones and boulders on shear surfaces, having emissions at 100 Hz to 1 MHz (*Lowell and Rose-Innes, 1980; Gershenzon and Bambakidis, 2001; Plewa and Plewa, 1992*). For deforming sliding bodies, emissions are generated by the formation of micro- and macro- cracks and fissures in the sliding body, having emissions up to 10 MHz (*Hanson and Rowell, 1980; Koltavy and Sikula, 2004; Rabinovitch et al., 2000a, 2000b; Takeuchi and Nagahama, 2006*). *Rabinovitch et al. (1998)* described the radio emission energy at the formation of cracks as follows:

$$A = A_0 \sin [\omega(t - t_0)] \left[ 1 - \exp \left( -\frac{(t - t_0)}{\tau} \right) \right], \quad t < T, \quad (2)$$

$$A = A_0 \sin [\omega(t - t_0)] \exp \left( -\frac{(t - T)}{\tau} \right) \left[ 1 - \exp \left( -\frac{(T - t_0)}{\tau} \right) \right], \quad t \geq T,$$

$A(t)$  being the pulse energy, where  $A_0$  is the peak pulse (maximum amplitude),  $\omega$  is the frequency,  $t_0$  is the pulse generation time,  $\tau$  is the pulse rise and fall time from the maximum and  $T$  is the pulse time during the amplitude maximum. When a sliding deforming body is porous (Fig. 2), emissions are generated by a flowing liquid representing an electrolyte driven by voltage changes, forming an electrical bilayer (*Mastow et al., 1989b; Pride and Morgan, 1991; Reppert et al., 2001; Adler 2001; Eccles et al., 2005; Heister et al., 2005*). This mechanism is typical of clays (*Fedorov et al., 2001; Kormiltsev et al., 1998*). Creeping deformations on clays are detectable at speeds from 4 mm/day (*Mastow et al., 1989b*).



The aim of our measurements is the verification of the applicability of the VLF receiver for monitoring the activity in the landslide body and finding the pattern in the radio spectrum, the Fast Fourier Transform (FFT) pattern, which is a pattern of the signal coming from the geological environment, due to compression of quartz clusters and other above-mentioned phenomena. Another benefit expected is the set-up of geophysical methodology for detecting the emissions using air-loop coils. The focus of the work will be to determine the possibility of the application of radio-geophysical surveys to predict adverse geodynamic phenomena in areas affected by landslides.

## 2. Material and methods

### 2.1. Field work

Fieldwork includes campaign and continuous measurements of EM emissions at selected locations in active landslide areas. Measurements are performed by sound cards such as an AD/DA converter, which consists of receiving antennas: dipole-electrodes, air-loop coils. In the case of air-loop coils, a sound card in the audio band 100 Hz – 24 kHz (stationary system) and 100 Hz – 91.5 kHz (mobile system) is used as the radio receiver (Fig. 3). The first air-loop assembly will be used as a stationary with continuous operation on the surface and will serve for continuous recording of radio emissions and subsequent correlation with the amount of precipitation, temperature changes and deformation in the landslide body.

It will also be used to separate noise caused by human activity, to eliminate anthropogenic noise. Monitoring of EM emissions took place in the ELF (extreme low frequency) and VLF (very low frequency) bands (cf. *Mastow et al., 1989b*), as well as in the HF (high-frequency) bands. The second assembly, located in the borehole, is similar, but instead of an air-loop coil (Figs. 3 and 4), it uses a miniWhip-type antenna. It has a relatively wide receiving range with 10 kHz – 30 MHz and has a suitable size for use in boreholes, similar to the method of PEE (*Vybiral, 2002*), where in contrast to PEE, it will be able to see the whole range in the form of a FFT spectrum of wider range from 10 kHz to 2 MHz bandwidth with Software Defined Radio (SDR) and soundcard. The description of the use of a miniWhip

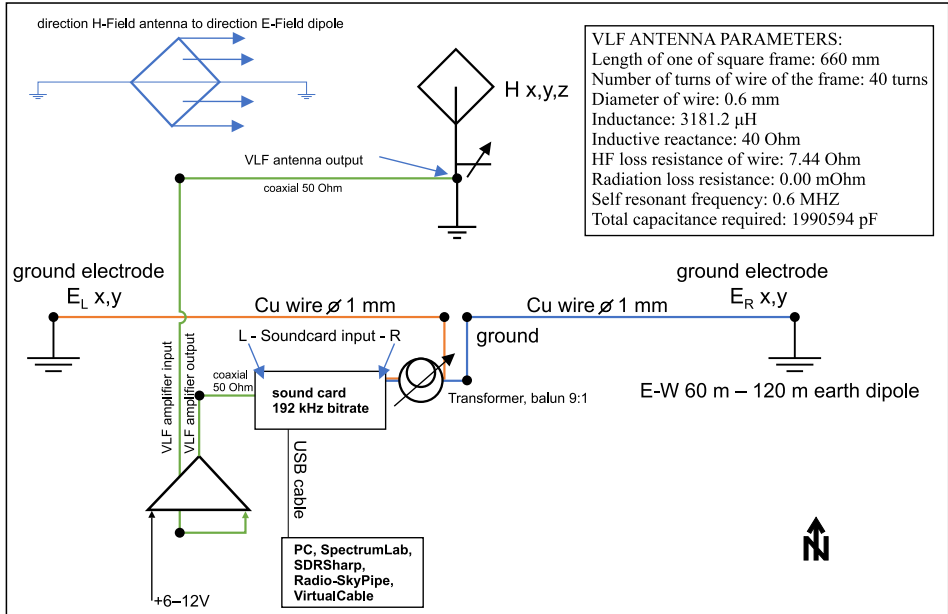


Fig. 3. Layout diagram of antenna elements and amplifiers of the VLF-HF monitoring station system.

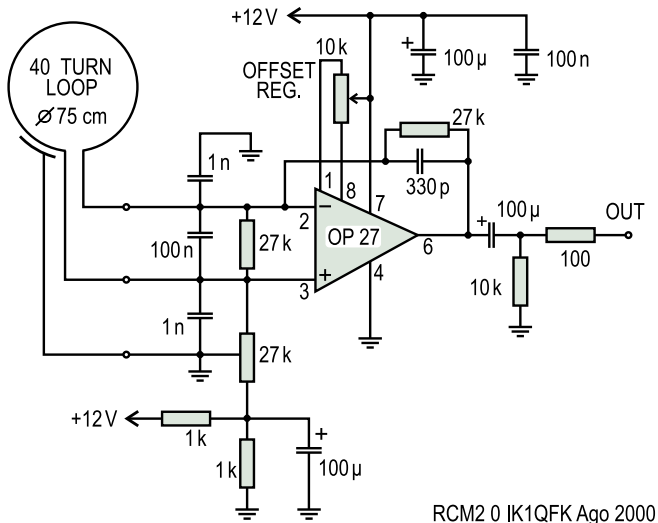


Fig. 4. Wiring diagram of the used VLF antenna system amplifier (source: <http://www.vlf.it/>).

antenna in boreholes is beyond the scope of this work and will be published in follow-up work.

The system consists of two systems, one antenna measuring the magnetic field, the coil, and the second measuring the electric field perpendicular to the magnetic field, using ground electrodes. The sound card has two inputs, L (left) and R (right). L is the input for the magnetic component and R is the input for the electrical component from the ground dipole.

Both are tracked together on a split spectrum for the L and R channels synchronously. The time control in the field comes from GPS time via USB input.

## 2.2. Data processing

We display the measured geo-electromagnetic field in the form of a “water-fall” image processed by FFT. The colour intensity of the colour scale lines corresponds to the signal intensity on a given frequency line. Signals originating from a natural source do not have the character of narrowly bounded frequency lines in the spectrum, but rather have the form of “clouds”, unbounded shapes with an irregularly changing frequency without modulation. Thus, natural sources of EM signals form radio signals without modulation at different frequencies in a certain wider spectrum than VLF, LF, and HF.

The observation system records a continuous spectrum in the VLF range, specifically from 100 Hz to 24 kHz, using air-loop antennas and an external sound card with 48 kHz sampling (stationary system). We can change the frequency of the measuring system at will. The device is controlled remotely via a remote desktop application. This whole system with measurements in the VLF and HF area is considered stationary and will serve as a reference station. With the same antenna configuration, field measurements will be performed in the landslide area as well as in the boreholes. We will correlate all measured data with meteorological and geophysical data and with geodetically measured movements and real deformations in the sliding body.

## 3. Results

So far, we have managed to build a network of two monitoring stations that operate continuously. Daily they record changes in the EM field ( $H + E$

field separately) in the area of active slope deformations on the western edge of the Nitra Uplands. Signals that attribute to the geological source were captured. The successful capture of landslide-related signal fulfils the first objective.

These signals were compared with sample signals, which were obtained by studying the older literature (*Mastow et al., 1989a; Blaha and Duras, 2004*). Furthermore, it is necessary to collect as many types as possible of patterns of spectral anomalies corresponding to EM emissions in the VLF–HF band due to geodynamic activity, and to compile a catalogue of radio spectral patterns (Figs. 5 and 6).

The position of pins (stakes) that were mounted on the nearby sliding body about 1 km from the village centre, where EM emissions are measured is reobserved in repeat campaigns (Fig. 7). After receiving the EM emissions, the distances between the marked pins are measured using a geodetic band. The distance must be measured at least on the same week as the

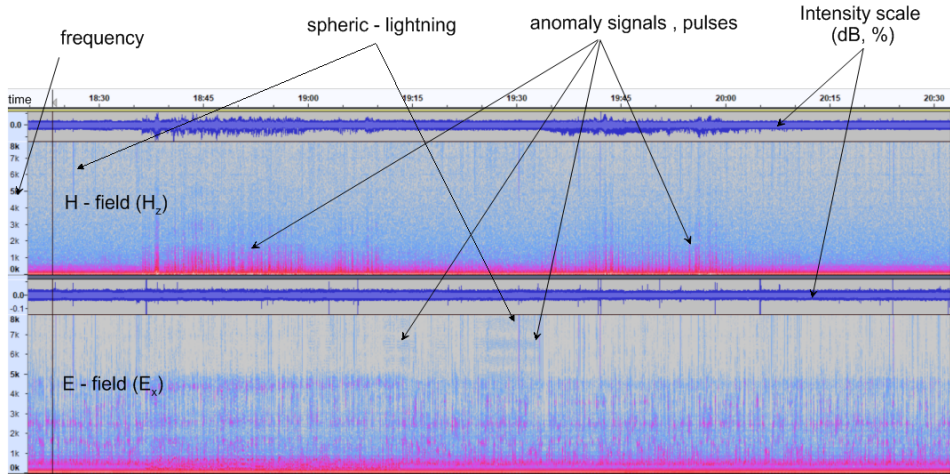


Fig. 5. VLF radio recording using the above equipment (Figs. 3 and 4) from the site Motocross, Vinohrady nad Váhom district, Galanta. The measurement took place on August 18, 2021 at 15:00 two days after a light rain up to 1 mm/hour. The recording took place at windless conditions at temperature 19 °C using an external sound card with 192 kHz sampling. The left channel is the magnetic component record and the right channel the electric component of the geoelectromagnetic field. Spherical signals (vertical lines), power grid noise (50 Hz – 250 Hz) and anomalous signals attributed to the geological source are visible on the spectral display.

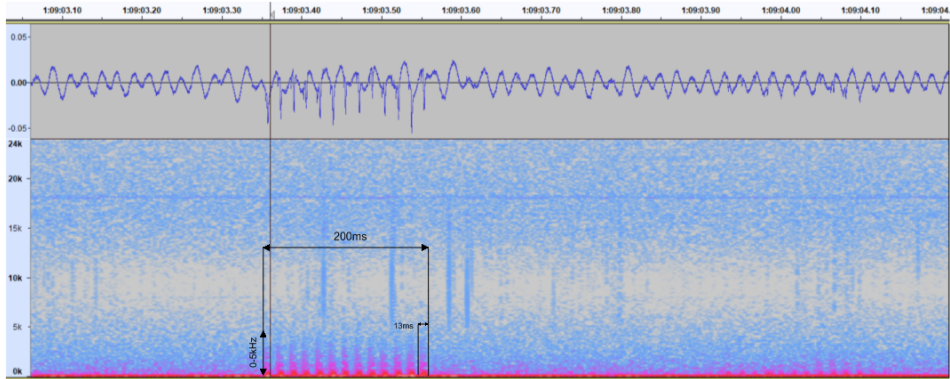


Fig. 6. Detail of the time period during pulses (in H field). A 5 kHz pulse (the maximum pulse intensity is from DC to 1 kHz) with a length of 13 ms and a group length of 200 ms with a pulse of 200 ms can be seen in the spectral record.

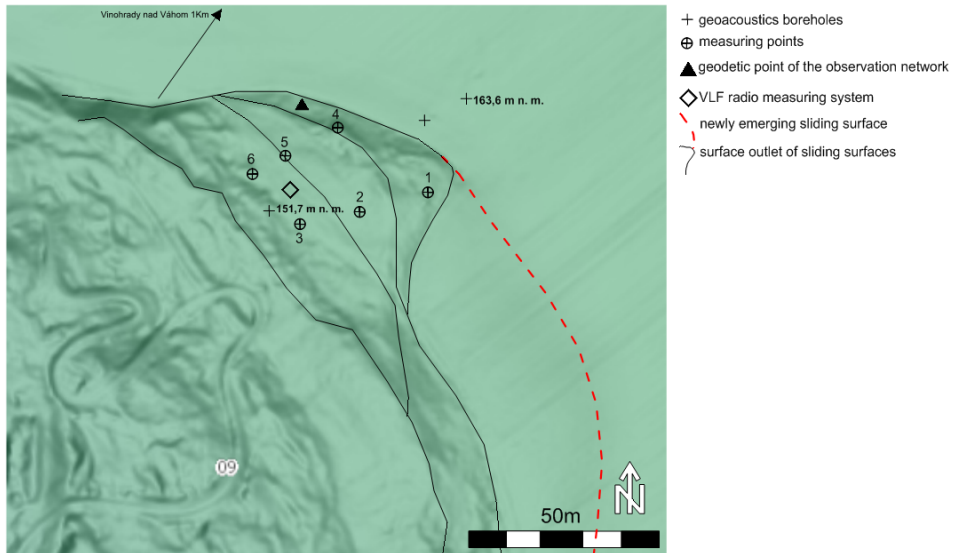


Fig. 7. Digital Terrain Model (DTM) of the sliding body with indication of the position of measuring pins, geodetic points for GPS measurement, geoacoustic boreholes suitable for future measurement of EM emissions in boreholes using E-field antenna (miniWhip). Surface penetrations of shear surfaces were derived from the DTM model and from direct in situ observations (DTM source: <http://www.zbgis.sk>).

radio emissions were measured. The EM emissions had the character of both pulsed and continuous EM emissions (Fig. 8).

The initialization distances between the individual pins were as follows:

- Distance between pins 1–2: 22.435 m on 25.9.2021 and on 3.10.2021. The displacement of 5 mm was measured on 23.11.2021.
- Distance between pins 2–3: 14.57 m on 25.9.2021 and on 3.10.2021. The displacement of 5 mm was measured on 23.11.2021.
- Distance between pins 4–5: 10.67 m on 25.9.2021 and on 3.10.2021. The displacement of 25 mm was measured on 23.11.2021.

A larger number of measurements is needed to validate the relationship between EM emissions and the deformation in the landslide body. The work ahead is the fieldwork scheduled for the spring of 2022, which will focus on more detailed measurements of deformations using drone photogrammetry and a GNSS network.

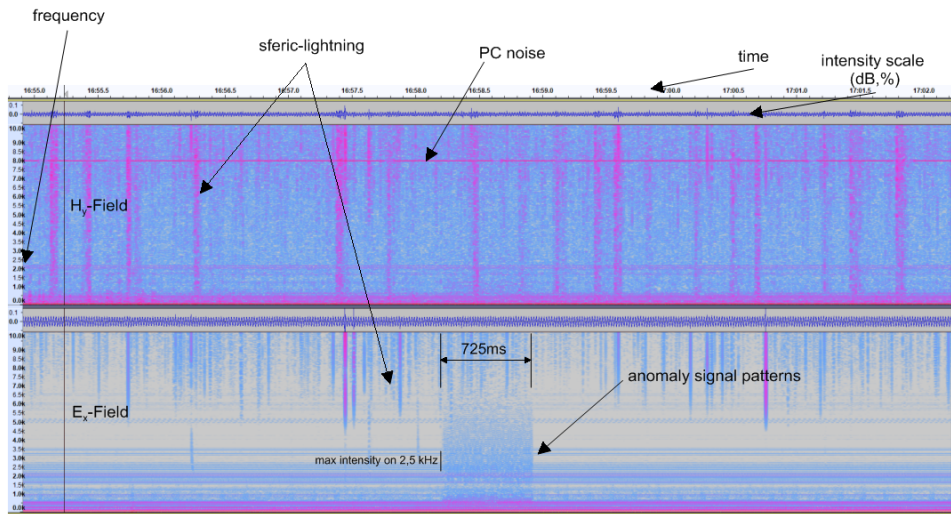


Fig. 8. Anomalous electromagnetic signal measured in the week during which there was a shift between the measuring points. The maximum shift was 2.5 cm/month in the northern part of the landslide. However, this is a relatively small deformation in the horizontal direction. We are missing vertical motion data. The signal has the character of a continuous emission with a duration of 725 ms. It was observed mainly in the electrical spectrum with a width of 10 kHz with a maximum intensity around 3 kHz.

#### 4. Discussion and conclusion

The aim of this preliminary work was to create a comparison network of VLF radio receivers in order to verify the possibility of monitoring slope deformations using VLF stations. Using a mobile station, which serves as the primary (Fig. 3), with respect to two static comparison stations, signals were recorded at selected sites in the landslide zone Sered' – Hlohovec.

The captured signals were of various natures from pulsed and periodic to continuous. They were recorded as 32-bit “.wav” files with 192 kHz sample rate (in case of mobile system in the field) sampling on the hard disk and subsequently analysed using the Audacity audio software. The recording always lasted for one battery discharge of the recording computer. The computer cannot be charged, or other electronic devices used, that could generate false anomalous signals during recording. Care must also be taken to properly switch off the motor vehicle and its electronic components when used as a mobile base. From a number of anomalous signals, we selected one specific signal (Figs. 5, 6, and 8), which does not have the nature of an antropogenic signal, artificially generated by human activity, as well as does not come from ionospheric disturbances. According to the frequency range (1 kHz – 6 kHz), these are not atmospheric discharges, such as due to lightning, which have their maximum intensity in the 11 kHz band, even if this signal is spherical. To eliminate the possibility of pollution of the sought signal by any possible artificial noise (the unwanted microphone effect), we tried to create artificial signals using various mechanical and electrical tools, but without success. We also exposed the measuring system to shocks and strong winds, but even then we did not manage to artificially create a similar spectral pattern. In addition, we managed to measure these anomalies only in the area of active landslides, where the deformation due to the movement of slope masses is visible. This strengthens the case for our hunted signal to be generated by the landslide activity. Additional anomalous spectral patterns from various landslide sites will be the subject of our further work.

**Acknowledgements.** I would like to thank the reviewers Peter Fabo, Ján Vozár and Fridrich Valach for their valuable comments that helped to improve the manuscript. This work was carried out with partial support of the Vega grant agency under project No. 2/0006/19.

## References

- Adler P. M., 2001: Macroscopic electroosmotic coupling coefficient in random porous media. *Math. Geol.*, **33**, 1, 63–93, doi: 10.1023/A:1007562326674.
- Blaha P., Duras R., 2004: Natural high frequency electromagnetic field on the Karolinka landslide. *EGRSE, Explor. Geophys. Remote Sens. Environ.*, **XI**, 1–2, 30–32.
- Eccles D., Sammonds P. R., Clint O. C., 2005: Laboratory studies of electrical potential during rock failure. *Int. J. Rock Mech. Min. Sci.*, **42**, 933–949, doi: 10.1016/j.ijrmmms.2005.05.018.
- Fabo P., Gajdoš V., Blaha P., 2004: The sources of 14 kHz EM fields observed at geoelectrical measurements. *EGRSE, Explor. Geophys. Remote Sens. Environ.*, **XI**, 1–2.
- Fedorov E., Pilipenko V., Uyeda S., 2001: Electric and magnetic fields generated by electrokinetic processes in a conductive crust. *Phys. Chem. Earth, Part C: Solar, Terrestrial & Planetary Science*, **26**, 10–12, 793–799, doi: 10.1016/S1464-1917(01)95027-5.
- Gershenson N., Bambakidis G., 2001: Modeling of seismo-electromagnetic phenomena. *Russ. J. Earth Sci.*, **3**, 4, 247–275, doi: 10.2205/2001ES000058.
- Hanson D. R., Rowell G. A., 1980: Electromagnetic radiation from rock failure. Report of Investigation no. 8594, Colorado School of Mines, Colorado, USA.
- Heister K., Kleingeld P. J., Keijzer T. J. S., Loch J. P. G., 2005: A new laboratory set-up for measurement of electrical, hydraulic and osmotic fluxes in clays. *Eng. Geol.*, **77**, 3-4, 295–303, doi: 10.1016/j.enggeo.2004.07.020.
- Jarošević A., Kundráčik A., 2004: Measurement of the natural high-frequency magnetic field (PEE) in the boreholes using FJV99 selective picoteslameter. *EGRSE, Explor. Geophys. Remote Sens. Environ.*, **XI**, 1-2, 8–12.
- Kharkhalis N. R., 1995: Manifestation of natural electromagnetic pulse emission on landslide slopes. *Geophys. J.*, **14**, 4, 437–443.
- Koktavy P., Sikula J., 2004: Physical model of electromagnetic emission in solids. In: *Proc. 26th Eur. Conf. Acous. Emission Testing, EWGAE 2004*, Berlin, Germany.
- Kormiltsev V. V., Ratushnyak A. N., Shapiro V. A., 1998: Three dimensional modeling of electric and magnetic fields induced by the fluid flow in porous media. *Phys. Earth Planet. Inter.*, **105**, 3-4, 109–118, doi: 10.1016/S0031-9201(97)00116-7.
- Krumbholz M., 2010: Electromagnetic radiation as a tool to determine actual crustal stresses – applications and limitations. PhD. thesis, Mathematisch-Naturwissenschaftlichen Fakultäten, Georg-August-Universität Göttingen.
- Lowell J., Rose-Innes A. C., 1980: Contact electrification. *Adv. Phys.*, **29**, 6, 947–1023, doi: 10.1080/00018738000101466.
- Maniak K., 2015: Measuring Electromagnetic Emissions from Active Landslides. *J. Telecommun. Inf. Technol.*, 2015/ 2, 44–51.
- Hayakawa M., 2015: Earthquake prediction with radio techniques. John Wiley & Sons, Singapore Pte. Ltd., ISBN: 978-1-118-77016-0, p. 125.
- Mastow R. Sz., Jaworowicz W. L., Gold R. M., 1989a: Electromagnetic activity during rock fracture (Elektromagnitnaja aktiwnost pri reologiczeskich ispitaniach gornych

- porod). *Engineering Geology (Inzenernaja Geologia)*, 2/1989, 121–124 (in Russian).
- Mastow R. Sz., Rudko G. I., Salomatin W. N., 1989b: Electromagnetic activity in clay landslides (Elektromagnitnaja aktiwnost pri razwitii opolzniei glinistych otłozheniach). *Engineering Geology (Inzenernaja Geologia)*, 6/1989, 119–122 (in Russian).
- Plewa M., Plewa S., 1992: *Petrophysics (Petrofizyka)*. Warsaw: Wydawnictwa Geologiczne, 326 p. (in Polish).
- Pride S. R., Morgan F. D., 1991: Electrokinetic dissipation induced by seismic waves, *Geophysics*, **56**, 7, 914–925, doi: 10.1190/1.1443125.
- Rabinovitch A., Frid V., Bahat D., 1998: Parametrization of electromagnetic radiation pulses obtained by triaxial fracture of granite samples. *Philos. Mag. Lett.*, **77**, 5, 289–293, doi: 10.1080/095008398178444.
- Rabinovitch A., Frid V., Bahat D., Goldbaum J., 2000a: Fracture area calculation from electromagnetic radiation and its use in chalk failure analysis. *Int. J. Rock Mech. Min. Sci.*, **37**, 7, 1149–1154, doi: 10.1016/S1365-1609(00)00042-3.
- Rabinovitch A., Frid V., Bahat D., Goldbaum J., 2000b: Decay mechanism of fracture induced electromagnetic pulses. *J. Appl. Phys.*, **93**, 9, 5085–5090, doi: 10.1063/1.1562752.
- Reppert P. M., Morgan F. D., Lesmes D. P., Jouniax L., 2001: Frequency dependent streaming potentials. *J. Colloid Interface Sci.*, **234**, 1, 194–203, doi: 10.1006/jcis.2000.7294.
- Takeuchi A., Nagahama H., 2006: Electric dipoles perpendicular to a stick-slip plane. *Phys. Earth Planet. Inter.*, **155**, 3-4, 208–218, doi: 10.1016/j.pepi.2005.12.010.
- Vybiral V., 2002: The PEE method helps assess slope stability. *Laboratory and Field Observations in Seismology and Engineering Geophysics*, Institute of Geonics of the AS CR, Ostrava-Poruba, Czech Republic.